

Application of the Diagrams of Phase Transformations during Aging for Optimizing the Aging Conditions for V1469 and 1441 Al-Li Alloys

Eva A. Lukina, Aleksander A. Alekseev, Vladislav V. Antipov, Denis V. Zaitsev, and Yuliya Yu. Klochkova

All-Russia Scientific Research Institute of Aviation Materials, Radio str. 17, Moscow, 105005 Russia

To describe the changes in the phase composition of alloys, it is convenient to construct TTT diagrams on the temperature-aging time coordinates in which time-temperature regions of the existence of nonequilibrium phases that form during aging are indicated. As a rule, in constructing the diagrams of phase transformations during aging (DPTA or TTT), time-temperature maps of properties are plotted. A comparison of the diagrams with maps of properties allows one to analyze the effect of the structure on the properties. In this study, we analyze the DPTAs of V1469 (Al - 1.2Li-0.46Ag-3.4Cu-0.66Mg) and 1441 (Al-1.8 Li-1.1 Mg-1.6 Cu, $C_{Mg}/C_{Cu} \sim 1$) alloys (wt%). Examples of the application of DPTA for the development of steplike aging conditions are reported.

Keywords: X-ray, TEM, T'_1 (Al_2LiCu), Ω' phase, Diagram of Phase Transformations during Aging

1. Introduction

Aluminum-based alloys with lithium take up a special position among other aging aluminum alloys. This is due to their high modulus of elasticity and low density, i.e., the properties that open up wide opportunities for the application of light metallic materials in the aerospace industry. When developing and optimizing the aging conditions, the time-temperature ranges of the existence of individual phases that form during aging should be available. For this purpose, it is convenient to use the diagrams of phase transformations during aging (DPTA), which are constructed in the temperature (t)-aging time (τ) coordinates [4, 5]. These diagrams are convenient in using them together with time-temperature maps of main mechanical properties ($\sigma_{0.2}$, σ_B , and δ), which were plotted for the same time-temperature range.

This work deals with studying the phase composition of 1441 and V1469 alloys and constructing DPTAs for these alloys in order to optimize single-stage aging conditions and to form criteria for the development of multistage aging conditions.

2. Materials and methods

We studied sheets of 1441 (Al-1.8 Li-1.1 Mg-1.6 Cu) and V1469 (Al-1.2 Li-0.46 Ag-3.4 Cu-0.66 Mg) alloys 2 and 3 mm thick, respectively. X-ray diffraction (XRD) studies were performed using a D/MAX-2500 (RIGAKU) diffractometer and monochromatized CuK_α radiation. Standard X-ray diffraction analysis was performed at 30 kV and 10 mA (operating conditions), and the scanning range was $2\theta = 15-90^\circ$. Electron microscopic studies (transmission electron microscopy (TEM)) were performed using a JEM-200CX (JEOL) transmission electron microscope. To determine the morphology and crystallographic parameters, dark-field image diffraction techniques were used.

3. Results

3.1 Diagram of Phase Transformations during Aging for the V1469 Alloy

The mechanical properties of the alloy were determined and time-temperature maps were plotted (Fig. 1). The lines corresponding to the same values of the properties, such as σ_B , $\sigma_{0.2}$, and δ , are in

the form of C curves. The regions of a so-called topographic ridge or the regions corresponding to the maximum strength properties ($\sigma_{0.2} = 550$ MPa) coincide with the region of a topographic valley (see Fig. 1b) or the region corresponding to the minimum plasticity ($\delta < 7\%$).

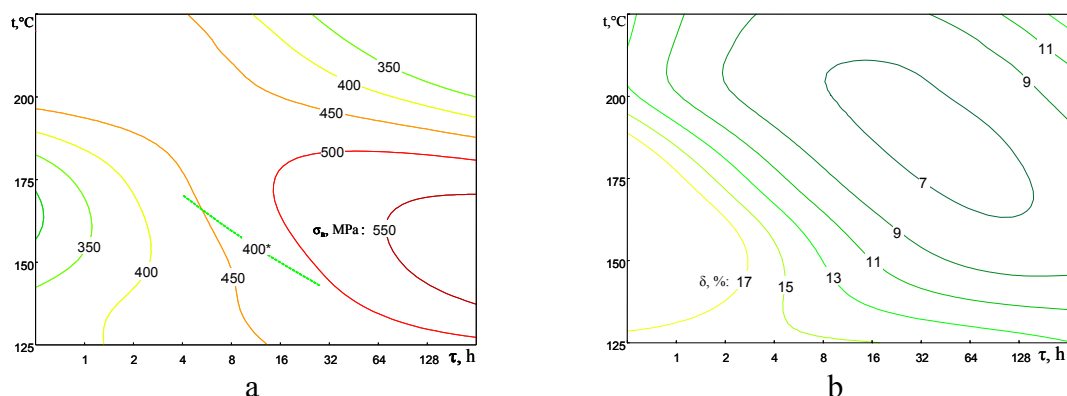


Fig. 1. Maps of mechanical properties (C curves) of V 1469 alloy sheets: (a) yield strength $\sigma_{0.2}$; and (b) elongation δ . Dashed lines indicate the level of straight characteristics for samples subjects to prolonged natural aging.

The yield strength of the samples aged at temperatures below 140°C after 1-year aging is lower than that of the as-quenched samples aged under the same conditions (see C curves for $\sigma_{0.2} = 400$). Therefore, preliminary natural aging affects the level of mechanical properties of the V1469 alloy aged under low-temperature conditions (up to 140°C). In this paper, we report data on the structure and properties of the V1469 alloy sheets aged under high-temperature conditions. The processes occurring during low-temperature aging call for a further investigation. The phase composition of the alloy at the overaging stage was determined by XRD analysis of the V1469 alloy sheets. In particular, the following phases are typical of aging at 225°C for 128 h, 200°C for 256 h, 150°C for 32 h, and 150°C for 64 h: $T_2(\text{Al}_6\text{Li}_3\text{Cu})$, $T_1(\text{Al}_2\text{LiCu})$ and $\theta(\text{Al}_2\text{Cu})$. To refine the time-temperature regions of the existence of nonequilibrium phases, we performed electron microscopic studies of the structure of the alloy aged under conditions selected with allowance for time-temperature maps of mechanical properties for the regions corresponding to the maximum properties, overaging, and underaging. At 200°C, lithium in Al-Li alloys (with 1.2% Li) [1,6] (V1469 alloy is among them) is mainly present in the form of a solid solution. Therefore, the δ' phase typical of all Al-Li alloys is formed in the V1469 alloy only at the low-temperature aging stage. In the high-temperature aging range, the δ' phase is almost absent. The principal peculiarities of high-temperature aging of the V1469 alloy are determined by intense decomposition of the solid solution inside grains and along subgrain boundaries with the formation of the Ω' phase. This phase contains silver (Fig. 2a) [7].

Electron diffraction studies of the Ω' phase show that thin diffuse streaks, which correspond to platelike precipitates several monatomic layers in thickness, form along all $\langle 111 \rangle_a$ directions in the $\langle 110 \rangle$ and $\langle 112 \rangle$ zone axes (see electron the diffraction pattern in Fig. 2a). Analogous diffraction effects are typical of the T_1 phase (Al_2LiCu) that precipitates during aging of Al-Li-Cu alloys [6]. The time-temperature region of the existence of the Ω' phase is wide; after aging at 150°C for 1 h, at 125°C for 32 h, and at 150°C for 4 h, Ω' -phase particles are observed in the form of individual thin plates 1-5 nm thick with a $\{111\}$ habit plane. This region is likely to be a field of Ω' phase nucleation. The regions of the Ω' and δ' phases are different and meet only within a narrow time-temperature range. After aging at 225°C for 32 h, the Ω' phase is present in the form of plates 10-15 nm thick. Large precipitates of a phase having a mosaic structure are also observed inside grains; particles of this phase decorate high-angle boundaries and subgrain boundaries. These precipitates are likely to correspond to the T_2 phase (Al_6CuLi_3).

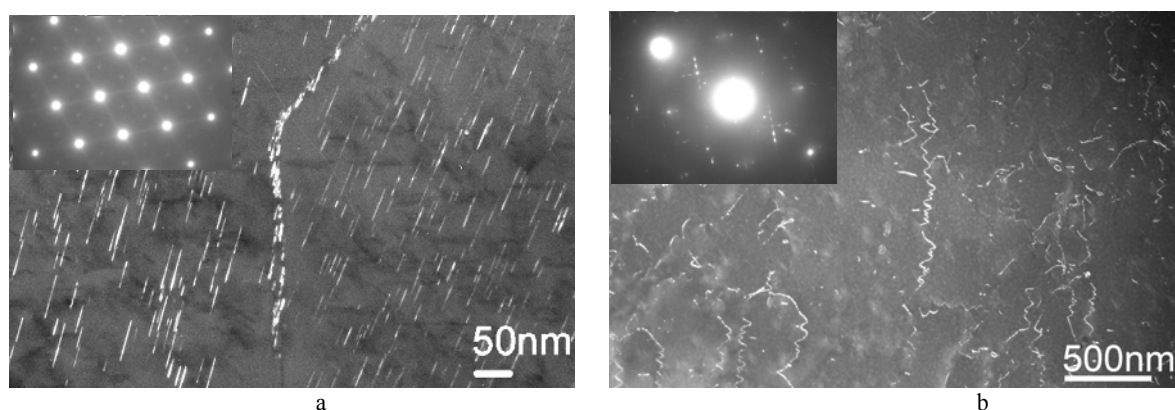


Fig. 2. Dark-field images of (a) Ω' phase, in the V1469 alloy after aging of 200°C for 4 h ($g = 1/2[111]$) and the associated $\langle 110 \rangle$ electron diffraction pattern (upper left corner) and (b) S' -phase particles ($g = 1/4[240]$) in the 1441 alloy and the associated $\langle 100 \rangle$ electron diffraction pattern (upper left corner).

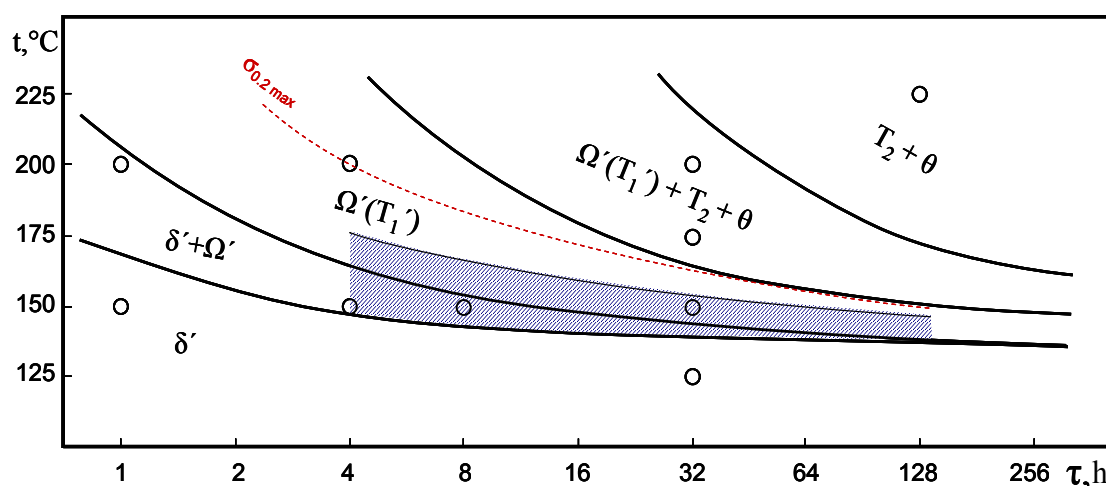


Fig. 3. Diagram of phase transformations during aging for the V1469 alloy. Points correspond to control conditions used for the structural studies. Lines indicate boundaries of phase regions. The plasticity-drop zone is shaded.

Thus, based on maps of mechanical properties and the XRD and electron microscopic data, the time-temperature regions of a number of phases, such as $((\alpha + \delta')$, $(\alpha + \delta' + \Omega' + \Omega'_{\text{hetero}})$, $(\alpha + \Omega' + \Omega'_{\text{hetero}})$, $(\alpha + T_2 + T_2_{\text{hetero}} + \Omega'(T_1) + T_1_{\text{hetero}} + \theta)$ were determined. The diagram of phase transformations during aging of the V1469 alloy was constructed (Fig. 3).

3.2 Diagram of Phase Transformations during Aging for the 1441 Alloy

We also determined the mechanical properties of the alloy and plotted time-temperature maps (Fig. 4). The region of the maximum properties ($\sigma_B \sim 430$ MPa, $\sigma_{0.2} \sim 370$ MPa), or a topographic ridge, was shown to correspond to the plasticity-drop zone ($\delta < 7\%$). Over-aging at different conditions was studied by XRD. The phase composition typical of this time-temperature region is $S'(Al_2CuMg)$, $T_1 (Al_2LiCu)$, and $T_2 (Al_6Cu(Li, Mg)_3)$. To perform electron-microscopic studies and take dark-field images, we used the maps of mechanical properties of the 1441 alloy and selected aging conditions corresponding to the maximum strength properties and the aging and overaging regions, namely, aging at 150°C for 32 h, 175°C for 4 h, 200°C for 4 h, 100°C for 8 h, 125°C for 32 h, and 200°C for 256 h. The phase composition and character of decomposition (homogeneous or heterogeneous) were refined and the boundaries of time-temperature regions of nonequilibrium

phases were determined. The δ' phase (Al_3Li) that is typical of the majority of Al-Li alloys is the main strengthening phase for the 1441 alloy. The presence of spherical δ' -phase particles, which are distributed homogeneously in the grain volume, is observed for all states under study. As the aging time or temperature increases, the particle size increases; the particle distribution in the volume remains uniform. At the late stages of aging (at 200°C for 256 h), the coarsening of δ' -phase precipitates and their partial dissolution are observed. Moreover, the S' phase (Al_2CuMg) forms in the 1441 alloy during aging [8]. The most convenient orientation for dark-field image studies of the S' phase is the crystallographic $\langle 001 \rangle$ zone axis (Fig.2b). Particles of this phase are observed in the form of rods that are arranged along $\langle 200 \rangle_\alpha$ directions and have a $\{120\}$ habit plane; the particles precipitate both in the grain volume and at dislocations. A comparison of the time-temperature regions of the S' and δ phases with the maps of mechanical properties of the 1441 alloy indicates a favorable effect of these phases on the formation of properties.

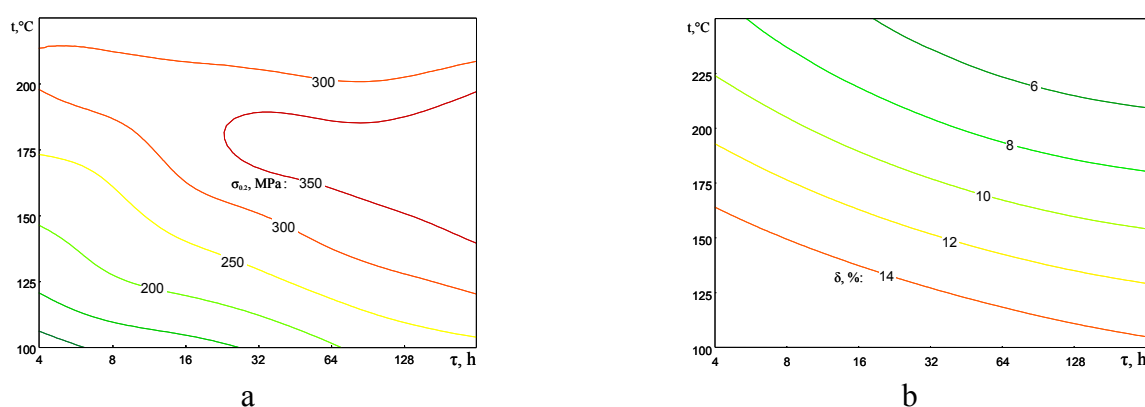


Fig. 4. Maps of the mechanical properties (C curves) of 1441 alloy sheets: (a) yield strength $\sigma_{0.2}$ and (b) elongation δ .

High-temperature aging is also characterized by the precipitation of T'_1 phase (Al_2LiCu) plate-like particles with a $\{111\}$ habit plane [2]. The most convenient orientation for the dark-field image studies of the T'_1 phase is the $\langle 110 \rangle$ crystallographic zone axis, which contains diffuse streaks along $\langle 111 \rangle_\alpha$ directions. As the plate thickness increases during aging, bulbs form at the streaks. The tendency toward heterogeneous nucleation at grain boundaries and subboundaries is typical for the precipitates of this phase. A comparison of the XRD data and the maps of properties indicates that the plasticity drop (δ) is related to intense formation of the T'_1 phase at grain and sub-grain boundaries. After aging at 150°C for 32 h, the decomposition at high-angle boundaries with the formation of T_2 -phase precipitates ~ 50 nm in size and a zone free from δ' -phase precipitates along a boundary is observed. Thus, based on the maps of mechanical properties and the results of structural studies, the time-temperature regions of a number of phases, such as $((\alpha + \delta')$, $(\alpha + \delta' + T_2 \text{ hetero})$, $(\alpha + \delta' + S' + T_1 + T_2 \text{ hetero})$, and $(\alpha + S' + T'_1 + T_1 + T_2 \text{ hetero})$, were determined. The diagram of phase transformations during aging was constructed for the 1441 alloy (Fig. 5). It was found based on the DPTA and the maps of mechanical properties for the 1441 alloy that the aging conditions used in practice, namely, aging at 150°C for 30 h correspond to the time-temperature region of underaging. In this study, we suggest three-stage aging conditions, namely, 150°C for 32 h + 175°C for 10 h + 120°C for 48 h. At the first stage of aging, a large amount of the δ' phase and a sufficient amount of the S' phase form. At the second stage, the amount of the S' phase increases; it is important to increase the efficiency of strengthening with δ' -phase precipitates without the formation of T'_1 phase particles. Excess equilibrium lithium is removed during low-temperature aging (third stage of aging), the conditions of which correspond to the time-temperature region of only the δ' phase. The conditions selected based of the DPTA allowed the properties of alloy to be improved. This is confirmed by a comparison of the mechanical properties of the 1441 alloys subjected to standard aging and aging the conditions of which were selected based on the DPTA: standard (150°C , 30 h) σ_B (430, MPa), $\sigma_{0.2}$ (300, MPa), δ (13.0%); step like σ_B (464, MPa), $\sigma_{0.2}$ (334, MPa), δ (13.3%).

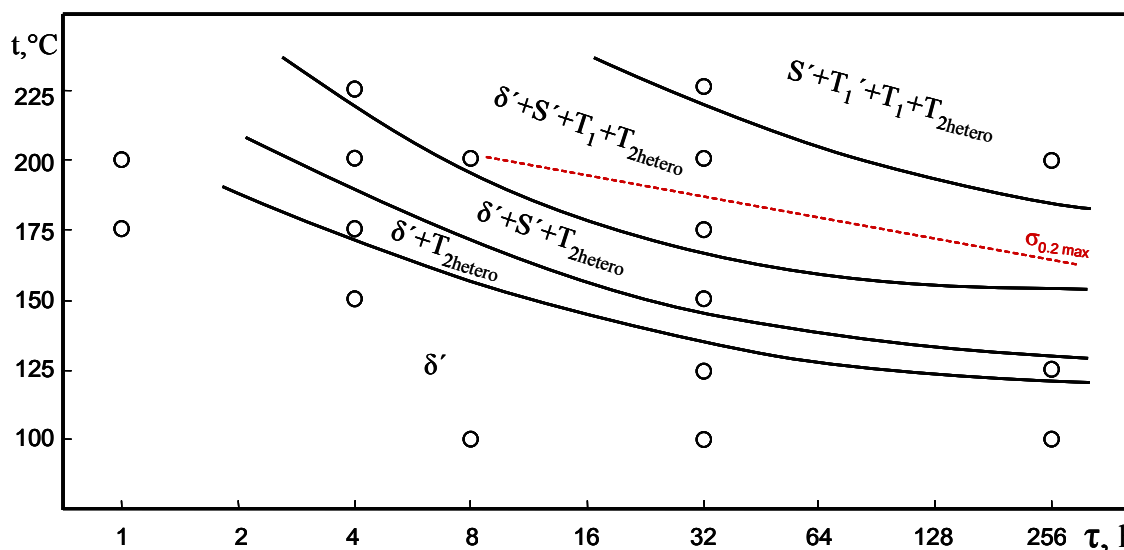


Fig. 5. Diagram of the phase transformations that occur during aging of the 1441 alloy. Points correspond to control conditions used for structural studies.

4. Conclusions

(1) Based on the diagram of phase transformations that occur during aging of the VI469 alloy, we found that the regions of the Ω' and δ' phases are different and meet only within a narrow time-temperature range. This is a feature of the VI469 alloy as compared to other Al-Li alloys.

(2) High- and low-temperature regions within which the properties of the VI469 alloy form in different ways were determined.

(3) The combinations of the strength and plasticity of the VI469 alloy is found to be controlled by the laws of Ω' -phase formation.

(4) Based on the constructed diagram of phase transformations during aging of the 1441 alloy and its comparison with the maps of mechanical properties, it was shown that the S' and δ' phases are favorable for the formation of the properties of the alloy.

(5) Phase analysis and the maps of mechanical properties of the 1441 alloy demonstrate that plasticity drop δ is related to intense formation of the T'_1 phase along grain and subgrain boundaries.

References

- [1] I. N. Fridlyander, K. V. Chuistov, A. L. Berezina, and N. I. Kolobnev: *Al-Li Alloys (Structure and Properties)* (Naukova Dumka, Kiev, 1992) [in Russian].
- [2] A. A. Alekseev, V. N. Ananiev, L. B. Ber, and A. D. Shestakov: *Phase Transformations during Aging of the Al-Li-Cu-Mg-(Zr) Alloys* Fiz. Met. Metalloved. 77 (4), (1994) 120-130.
- [3] R. J. Chester and I. J. Polmer: *Precipitation in Al-Cu-Mg-Ag Alloys in The Metallurgy of Light Alloys*. Spring Residential Conference L. Institution of Metallurgists 18 (6), (1983) 75-81.
- [4] V. G. Davydov, L. B. Ber. E. Ya. Kaputkin, V. I. Komov, O. G. Ukolova, and E. A. Lukina: *TTP and TTT Diagrams for Quench Sensitivity and Ageing of 1424 Alloy*, Mater. Sci. Eng. A 280, (2000) 76-82.
- [5] A. A. Alekseev and L. B. Ber: *Diagrams of Phase Transformations during Aging of Al-Zn-Mg-(Cu), Al-Li-Cu, and Al-Li-Cu-Mg Alloys*, Tekhnol. Legk. Splavov, No. 5, (1991) 15-19.
- [6] L. F. Mondolfo: *Aluminum Alloys: Structure and Properties* (Butterworths, London, 1976; Metallurgiya, Moscow, 1979).
- [7] V. V. Teleshov and A. P. Golovleva: *Effect of Small Silver Additions and Preparation Technology Parameters on the Structure and Properties of Half-Finished Products of the Al-Cu-Mg-Ag-X_i-Alloys*, Tekhnol. Legk. Splavov, No. 1-2, (2006) 99-119.

- [8] A. A. Alekseev, V. N. Ananiev, L. B. Ber. and E. Ya. Kaputkin: *Structure of Strengthening Precipitates Formed during High-Temperature Aging of Al-Cu-Mg Alloys*, Fiz. Met. Metalloved. 76 (3), (1993) 81-90.